Transactions on Soft Computing

www.tsc.reapress.com

Trans. Soft. Comput. Vol. 1, No. 3 (2025), pp. 203–216.

Paper Type: Original Article

Temporal Multilayer Fuzzy Quantum Graphs for Football Outcome Prediction and Player-Influence Ranking

Nivedita Kuity[1,*], Laxminarayan Sahoo[1]

[1]Department of Computer and Information Science, Raiganj University, Raiganj–733134, India; nivedita@raiganjuniversity.ac.in; lxsahoo@raiganjuniversity.ac.in.

Citation:

Received: 22 August 2024 *Revised: 14 October 2024* *Accepted: 20 December 2024*	Kuity, N., & Sahoo, L. (2025). Temporal multilayer fuzzy quantum graphs for football outcome prediction and player-influence ranking. *Transactions on soft computing*, *1*(3), 203-216.

Abstract

Identifying structurally influential football players and predicting match outcomes from player interactions are challenging because event networks are temporal and multi-relational. This study proposes a Temporal Multilayer Fuzzy Quantum Graph framework that combines fuzzy-weighted passing, defensive, possession, and spatial-progression layers with a continuous-time quantum walk. A real-symmetric aggregate adjacency matrix is used as the Hamiltonian so that the evolution is unitary. The framework is illustrated using event data from all 64 matches of the 2018 FIFA World Cup in StatsBomb Open Data. Fifteen-minute temporal windows are aggregated into player-level quantum centralities and team-level descriptors. In the supplied results, a random forest using fuzzy-quantum descriptors obtained a macro-AUC of 0.551, compared with 0.525 for a classical-centrality baseline, although its accuracy was lower. A World Cup Final case study ranked Paul Pogba highest among France players by the proposed structural centrality. These findings are exploratory: the attached source package contains neither executable analysis code nor fold assignments, so the reported predictive metrics require independent reproduction with match-grouped validation before publication. The framework is therefore presented primarily as an interpretable player-influence model, with outcome prediction as a preliminary application.

Keywords: Continuous-time quantum walk, Fuzzy graph, Multilayer network, Football analytics, Quantum centrality, StatsBomb.

1 | Introduction

Modern football analytics has been transformed by detailed event data, which record

Corresponding Author: nivedita@raiganjuniversity.ac.in
https://doi.org/10.48314/tsc.v1i3.69

passes, duels, shots, pressures, and related actions with timestamps and event locations. Unlike continuous player-tracking data, event data do not provide the simultaneous positions of every player. They nevertheless support network-based descriptions of team play, in which players are nodes and recorded interactions define weighted edges [1, Classical centrality measures and PageRank have been widely used to identify influential players in passing networks [3, 4]. Some of these measures are global rather than local; however, they are commonly applied to a single time-aggregated graph and do not model quantum interference between alternative interaction pathways. 2].

Quantum walks offer a principled way to capture such interference effects. A continuous-time quantum walk (CTQW) evolves a quantum state under a Hermitian Hamiltonian derived from a graph operator. Unlike a classical random walk, its node probabilities reflect constructive and destructive interference among paths [6, 7]. CTQW-based centrality measures have been explored in complex-network analysis [8, 9]. Their use here is quantum-inspired: the calculations are performed by classical matrix exponentiation and do not claim quantum-computational speedup.

Separately, fuzzy set theory can encode qualitative football concepts–such as high passing accuracy or low pressure–as graded, rule-based memberships rather than hard thresholds [10, 12]. The present framework combines fuzzy edge weighting with quantum-walk centrality on a temporal, multilayer representation of a match.

1.1 | Contributions

This paper makes the following contributions:

1. We formalize a fifteen-step Temporal Multilayer Fuzzy Quantum Graph (TMFQG) methodology that (i) builds four event-derived interaction layers per temporal window, (ii) fuzzifies edge weights, (iii) symmetrizes and combines the layers into a Hermitian Hamiltonian, (iv) evolves a CTQW, and (v) aggregates quantum centrality into team-level descriptors.
2. We implement the entire pipeline on real, open StatsBomb event data covering all 64 matches of the 2018 FIFA World Cup, producing 128 team-match observations and 1,408 player-match quantum centrality records.
3. We train and cross-validate a Random Forest match-outcome classifier on the resulting five-dimensional quantum feature vector, benchmarking it against Gradient Boosting, Logistic Regression, an RBF-kernel SVM, and a classical-centrality-only Random Forest baseline.
4. We present a World Cup Final case study in which the proposed structural centrality ranks Paul Pogba highest among the selected France players. This is an influence ranking, not a causal claim that one player decided the match.

Paper organization.

Section 2 reviews related work in network-based football analytics, quantum walks, and fuzzy graph theory. Section 3 presents the full TMFQG methodology. Section 4 describes the StatsBomb 2018 World Cup dataset and our event-to-graph mapping. Section 5 details the experimental setup. Section 6 reports quantitative results, including model comparison, ROC analysis, and feature importance. Section 7 presents the World Cup Final case study. Section 8 discusses findings, limitations, and threats to validity. Section 9 concludes.

2 | Related Work

Network analysis in football. Passing-network representations of football matches include the work of Duch et al. [13], Grund [1], and Peña and Touchette [2]. Later studies examined temporal network organization and the relation between network metrics and team performance [4]. Although many applications use static, single-layer, time-aggregated graphs, football-network research also includes explicitly temporal and multilayer formulations [5].

Multilayer and temporal networks. Multilayer network theory [14] generalizes single graphs to structures with multiple types of edges (layers) connecting a common node set, with inter-layer coupling parameters controlling how influence propagates across layers. Temporal network methods [15] further discretize interactions into time windows, allowing dynamic centrality measures to be computed. Both ideas have seen limited but growing use in sports analytics [16], motivating our four-layer (passing, defensive, possession, spatial), temporally windowed construction.

Quantum walks and quantum centrality. The continuous-time quantum walk was introduced by Farhi and Gutmann [6] as a quantum analogue of a classical continuous-time walk, evolving a state $|\psi(t)\rangle = e^{-iHt}|\psi(0)\rangle$ under a Hermitian Hamiltonian H. Childs [7] established the computational universality of CTQWs, and subsequent work used time-averaged CTQW probabilities as centrality measures on complex networks [8, 9]. The present work evaluates this type of measure on event-derived football networks.

Fuzzy graph theory in sports. Fuzzy set theory [10] and fuzzy graph theory [11] provide a principled way to represent graded, rule-based relationships. Tavana et al. [12] used fuzzy inference for player selection and team formation. Our edge-weighting scheme follows this tradition by using ramp memberships and a product t-norm to combine passing, pressure, and possession-context information before quantum evolution.

3 | Methodology

The proposed framework integrates fuzzy logic with Continuous-Time Quantum Walks on temporal, multilayer football interaction networks. Figure 1 illustrates the overall multilayer structure. The complete methodology consists of the following fifteen steps.

Step 1: Football match representation. Let $P = \{p_1, p_2, \ldots, p_n\}$ denote the selected players for one team. For each temporal window τ, four layer-specific interaction graphs are constructed:

$$G_\tau^{(\ell)} = (P, E_\tau^{(\ell)}), \qquad \ell = 1, \ldots, 4.$$

The four layers represent passing, defensive co-actions, possession co-occurrence, and spatial progression. Their event-to-edge mappings are specified in Section 4.

Step 2: Feature extraction. For each ordered player pair and temporal window, features

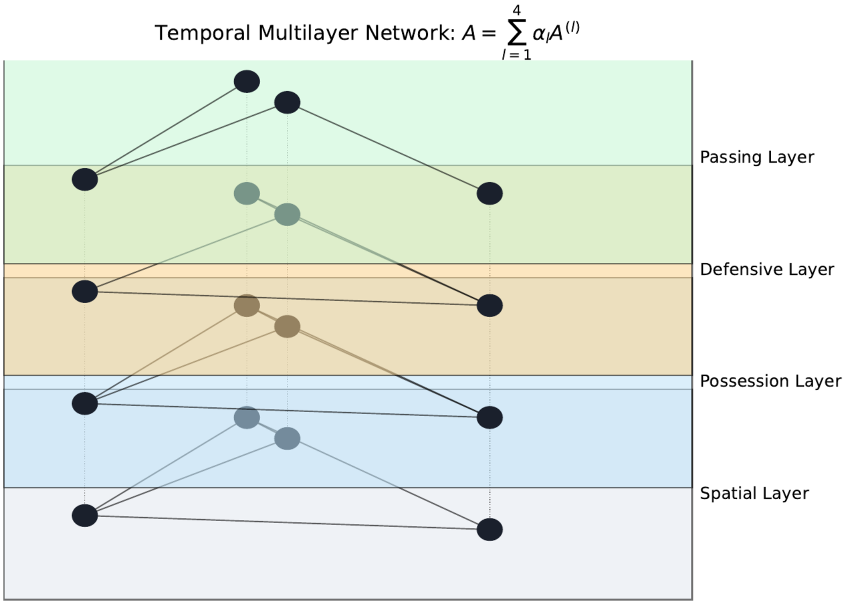

Figure 1. Schematic of the four-layer temporal network with layer weights α_ℓ.

are aggregated from fields available in the event records:

$$x_{ij}(\tau) = [\text{completion ratio}, \text{ low-pressure ratio}, \\ \text{possession co-occurrence}, \text{ normalized pass length}].$$

The completion ratio is computed from attempted passes with a named intended recipient. Expected goals (xG), which applies to shots rather than ordinary passes, and ball speed, which is not a direct tracking measurement in this event-only construction, are not used as pass-edge features.

Step 3: Fuzzy membership computation. Each aggregated numerical feature is transformed into a fuzzy membership. For example, if x is a pair-window pass-completion percentage, its high-accuracy membership is

$$\mu_H(x) = \begin{cases} 0, & x \leq 60, \\ \dfrac{x-60}{30}, & 60 < x < 90, \\ 1, & x \geq 90, \end{cases}$$

and analogous piecewise-linear functions define low and medium memberships (Figure 2). The low-pressure membership is computed from the fraction of relevant actions not marked by the StatsBomb `under_pressure` field. These thresholds are fixed modeling choices and should be tested in a sensitivity analysis.

Step 4: Fuzzy rule inference. The fuzzy inference engine evaluates predefined football rules,

$$R_1: \quad \text{IF pass accuracy is high and pressure is low,} \\ \text{THEN connection strength is very high.}$$

Additional rules govern the defensive, possession, and spatial-progression layers. The passing-layer edge weight uses the product t-norm,

$$w_{ij}^{(1)}(\tau) = \mu_{\text{accuracy}}\, \mu_{\text{low pressure}}\, \mu_{\text{possession}}, \qquad 0 \leq w_{ij}^{(1)}(\tau) \leq 1.$$

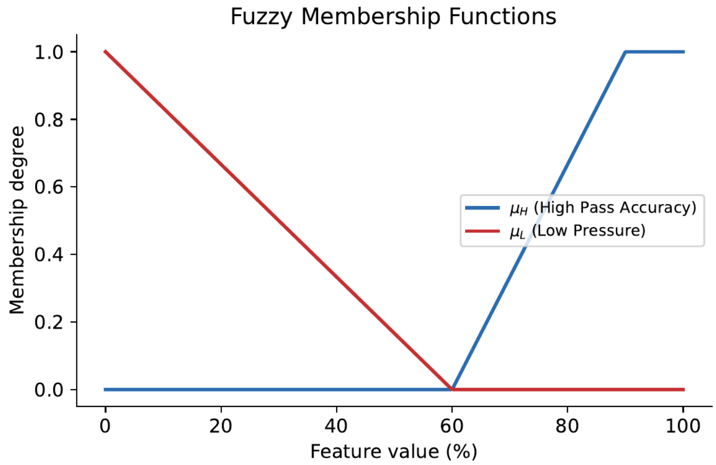

Figure 2. Fuzzy membership functions.

Step 5: Construction of the fuzzy adjacency matrix. The directed weighted adjacency matrix for layer ℓ and window τ is

$$B^{(\ell)}(\tau) = [b_{ij}^{(\ell)}(\tau)]_{n\times n}.$$

Because a CTQW Hamiltonian must be Hermitian, each layer is converted to a real-symmetric operator

$$A^{(\ell)}(\tau) = \frac{B^{(\ell)}(\tau) + B^{(\ell)}(\tau)^{\mathsf{T}}}{2}.$$

This symmetrization preserves interaction strength but discards edge direction; directed quantum-walk formulations are left for future work.

Step 6: Temporal multilayer network construction. Four interaction layers are considered: $A^{(1)}$ (passing), $A^{(2)}$ (defensive), $A^{(3)}$ (possession), and $A^{(4)}$ (spatial progression). The combined real-symmetric adjacency matrix is

$$A(\tau) = \sum_{\ell=1}^{4} \alpha_\ell A^{(\ell)}(\tau), \qquad \alpha_\ell \geq 0, \quad \sum_{\ell=1}^{4} \alpha_\ell = 1.$$

The implementation uses $(\alpha_1, \alpha_2, \alpha_3, \alpha_4) = (0.45, 0.20, 0.20, 0.15)$. These weights were fixed before outcome modeling and were not tuned on labels; they should therefore be interpreted as a priori design choices rather than statistically optimized values.

Step 7: Hamiltonian construction. The spectral radius of the symmetric combined adjacency matrix is

$$\rho(A) = \max\{|\lambda_1|, |\lambda_2|, \ldots, |\lambda_n|\},$$

where the eigenvalues are real. For $\rho(A(\tau)) > 0$, the normalized Hamiltonian is

$$H(\tau) = \frac{A(\tau)}{\rho(A(\tau))}.$$

If $A(\tau) = 0$, set $H(\tau) = 0$. Thus $H(\tau)$ is Hermitian in every window and generates unitary evolution.

Step 8: Initialization of the quantum state. The quantum walker is initialized in an equal superposition over all players,

$$|\psi(0)\rangle = \frac{1}{\sqrt{n}} \sum_{i=1}^{n} |i\rangle = \frac{1}{\sqrt{n}} \begin{pmatrix} 1 \\ 1 \\ \vdots \\ 1 \end{pmatrix}.$$

Step 9: Continuous-time quantum walk. Within window τ, the quantum state evolves according to

$$|\psi_\tau(s)\rangle = e^{-iH(\tau)s}|\psi(0)\rangle, \qquad U_\tau(s) = e^{-iH(\tau)s}.$$

The exponential is evaluated numerically. Hermiticity implies $U_\tau(s)^* U_\tau(s) = I$ analytically; numerical implementations should verify that the unitarity residual remains within floating-point tolerance.

Step 10: Quantum transition probability. The probability of finding the walker at player i at evolution time s is $P_{i,\tau}(s) = |\psi_{i,\tau}(s)|^2$; the transition probability from i to j is $Q_{ij,\tau}(s) = |[U_\tau(s)]_{ji}|^2$.

Step 11: Quantum centrality computation. For sampled evolution times $s_1, \ldots, s_M$, the quantum centrality of player i within a window is

$$QC_i(\tau) = \frac{1}{M} \sum_{k=1}^{M} |\psi_{i,\tau}(s_k)|^2.$$

The reported implementation samples $M = 10$ dimensionless times uniformly on $s \in [0.5, 5.0]$. Spectral-radius normalization makes this range comparable across windows, but robustness to the sampling interval and number of samples remains to be evaluated.

Step 12: Temporal aggregation. For a match divided into T non-overlapping 15-minute windows, the overall influence score is

$$QC_i = \frac{1}{T} \sum_{\tau=1}^{T} QC_i(\tau).$$

Step 13: Team-level quantum features. Five quantities are recorded per team-match:

$$F_1 = \frac{1}{n} \sum_{i=1}^{n} QC_i, \qquad F_2 = \max_i QC_i,$$

$$F_3 = \frac{1}{n} \sum_i (QC_i - \overline{QC})^2,$$

$$F_4 = \frac{1}{n(n-1)} \sum_{i \neq j} \overline{Q}_{ij}, \qquad F_5 = \frac{1}{|E|} \sum_{(i,j) \in E} w_{ij}$$

where $\overline{Q}$ is averaged over the same evolution times and temporal windows used for QC_i; set $F_5 = 0$ in an empty-edge window. Since each quantum probability vector sums to one, $\sum_i QC_i = 1$ and therefore $F_1 = 1/n$ exactly when all windows use the same n players. Thus F_1 is a normalization diagnostic, not an informative predictor; the substantive descriptors are F_2–F_5.

Step 14: Match outcome prediction. The supplied experiment used $X = (F_1, \ldots, F_5)$ to train a supervised classifier for $Y \in \{\text{Win}, \text{Draw}, \text{Loss}\}$, with $\widehat{Y} = \arg\max_y P(Y = y \mid X)$. Retaining the constant F_1 does not add information, and future implementations should omit it or replace it with a nonconstant distributional descriptor such as normalized quantum-centrality entropy.

Step 15: Performance evaluation. Predictive performance is evaluated with Accuracy, macro-averaged Precision, Recall, F1, and one-vs-rest AUC-ROC. The proposed fuzzy quantum graph framework is compared against classical graph centrality measures computed on the equivalent aggregated network, to isolate the marginal value of the fuzzy-quantum construction.

4 | Dataset

StatsBomb Open Data: 2018 FIFA World Cup. We use the StatsBomb Open Data event feed for the 2018 FIFA World Cup (competition id 43, season id 3) [17], comprising 64 matches from the group stage through the Final. The records provide event actors, teams, timestamps, event locations, and event-specific attributes. Pass records include the intended recipient and spatial descriptors, and events may carry an `under_pressure` flag. These are event data, not continuous tracking coordinates for all players.

Event-to-graph mapping. We map raw events to the four interaction layers of Section 3 as follows:

- **Passing layer:** attempted passes with named intended recipients are used to compute pair-window completion and pressure ratios; completed passes contribute interaction counts. The pressure membership uses `under_pressure` as an event-level proxy.
- **Defensive layer:** defensive actions by two teammates within the same opponent-possession sequence contribute a co-action edge, weighted by action frequency. This is an event-sequence proxy, not measured simultaneous defensive coordination.
- **Possession layer:** players who touch the ball within the same StatsBomb possession chain receive a co-occurrence edge, capturing shared involvement in a coherent attacking or defensive sequence.
- **Spatial-progression layer:** completed passes contribute an edge weighted by normalized pass length and change in field position. Because simultaneous player locations are unavailable, this layer measures event-derived ball progression rather than inter-player spatial proximity.

Each team-match is restricted to the 11 players with the highest event-touch counts, giving 11×11 adjacency matrices. This selection can mix starters and substitutes and is therefore a modeling choice that requires sensitivity analysis. Matches are split into non-overlapping 15-minute windows: six regulation-time windows, with up to two additional windows for extra time; empty windows may be omitted.

Resulting corpus. After filtering matches with usable event data, the pipeline produced:

- **128 team-match observations** (two per match: home and away team), each with five quantum features F_1–F_5 and a ground-truth outcome label derived from the final score;

- **1,408 player-match centrality records** (11 players × 128 team-matches), each with quantum centrality alongside classical degree, eigenvector, betweenness, and PageRank centrality computed on the same aggregated network.

The outcome label distribution is 51 Wins, 51 Losses, and 26 Draws, reflecting the natural class imbalance of knockout-heavy tournament football.

5 | Experimental Setup

The supplied manuscript reports five-fold cross-validation for logistic regression, an RBF-kernel support-vector machine, random forest, and gradient boosting models, together with a random-forest baseline based on classical centralities. Accuracy and macro-averaged precision, recall, F1, and one-vs-rest AUC are reported.

The two team-level rows from the same match are statistically dependent and must remain in the same validation fold; otherwise, information from one side of a match may leak into training while the opposing side is evaluated. All preprocessing, feature scaling, and model selection must likewise be fitted within each training fold. The supplied package contains figures and summary tables but no executable analysis code, fold assignments, random seeds, or hyperparameter records. Consequently, the numerical results below are retained as author-supplied exploratory values rather than independently reproduced estimates. Before publication, the complete pipeline should be rerun with match-grouped folds and archived code.

6 | Results

6.1 | Model Comparison

Table 1 summarizes the author-supplied five-fold results. The random forest trained on fuzzy-quantum features has the highest reported macro-AUC (0.551), 0.026 above the classical-centrality baseline (0.525), while the classical baseline has the highest reported accuracy (0.477). No confidence interval or paired significance test is available, so the AUC difference should not be interpreted as established superiority.

Table 1. Author-supplied five-fold performance of match-outcome classifiers; independent reproduction is required.

Model	Accuracy	Precision	Recall	F1	AUC
Classical Centrality (RF)	0.477	0.320	0.399	0.355	0.525
SVM (RBF), quantum features	0.438	0.292	0.366	0.325	0.427
Logistic Regression, quantum features	0.430	0.350	0.366	0.342	0.494
Random Forest, fuzzy-quantum features	0.422	0.368	0.359	0.335	**0.551**
Gradient Boosting, quantum features	0.391	0.383	0.371	**0.375**	0.526
Random (3-class) reference	0.333	0.333	0.333	0.333	0.500

6.2 | ROC Analysis

Figure 3 shows the supplied one-vs-rest ROC curves for the fuzzy-quantum random forest. The Win class has the highest displayed AUC (approximately 0.59), while Draw has the lowest. Without stored fold predictions, uncertainty intervals cannot be reconstructed.

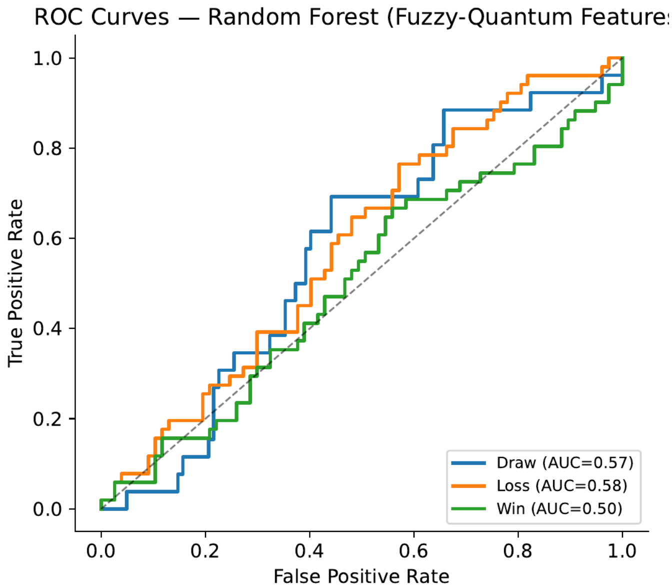

Figure 3. One-vs-rest ROC curves for the Random Forest model trained on fuzzy-quantum features F_1–F_5.

6.3 | Confusion Matrix

Figure 4 shows the supplied confusion matrix for the fuzzy-quantum random forest. The displayed predictions favor Win/Loss over Draw, consistent with the smaller Draw class (26 team-match rows versus 51 for each of Win and Loss).

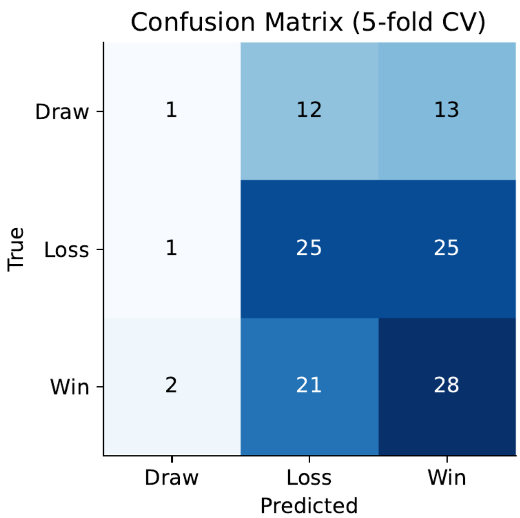

Figure 4. Confusion matrix for the fuzzy-quantum Random Forest.

6.4 | Feature Importance

Figure 5 shows the supplied Gini importances from a random forest fitted to the full dataset. Maximum quantum centrality (F_2) and average quantum connectivity (F_4) have the largest displayed importances. In exact arithmetic, $F_1 = 1/11 \approx 0.0909$ under the stated definition; the slightly different tabulated values indicate rounding, missing-window handling, or an implementation mismatch that must be reconciled. F_1 should have no predictive value once normalization is implemented consistently.

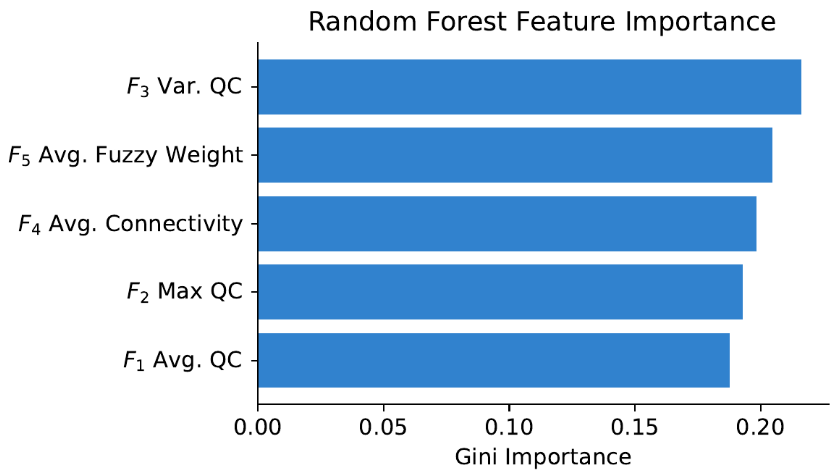

Figure 5. Random Forest Gini feature importance for the five fuzzy-quantum team-level features.

Table 2. Mean fuzzy-quantum feature values by match outcome (team-level, $n = 128$).

Outcome	F_1	F_2	F_3	F_4	F_5
Win	0.0914	0.1519	0.00071	0.0479	0.2257
Loss	0.0915	0.1469	0.00062	0.0478	0.2291
Draw	0.0915	0.1514	0.00071	0.0481	0.2293

Table 2 shows a small descriptive difference in F_2 between winning and losing teams (0.1519 versus 0.1469). No uncertainty estimate is supplied, so this difference is not evidence of a population-level association. The class means for F_1 should be identical under the mathematical definition and require implementation verification.

7 | Case Study: The 2018 World Cup Final

To illustrate structural player attribution, we present a case study of the 2018 FIFA World Cup Final (France 4–2 Croatia, Luzhniki Stadium, 15 July 2018).

Figure 6 shows France's full-match passing network, with node size and color encoding each player's time-averaged quantum centrality QC_i. Table 3 reports the ranked quantum centralities for all 11 most-involved France players.

Figure 7 plots the supplied CTQW probabilities for the four highest-ranked France players. The trajectories show oscillatory probability redistribution under unitary evolution; they are not physically damped. Pogba has the highest time-averaged score in this construction, but the ranking is structural and does not establish causal match decisiveness.

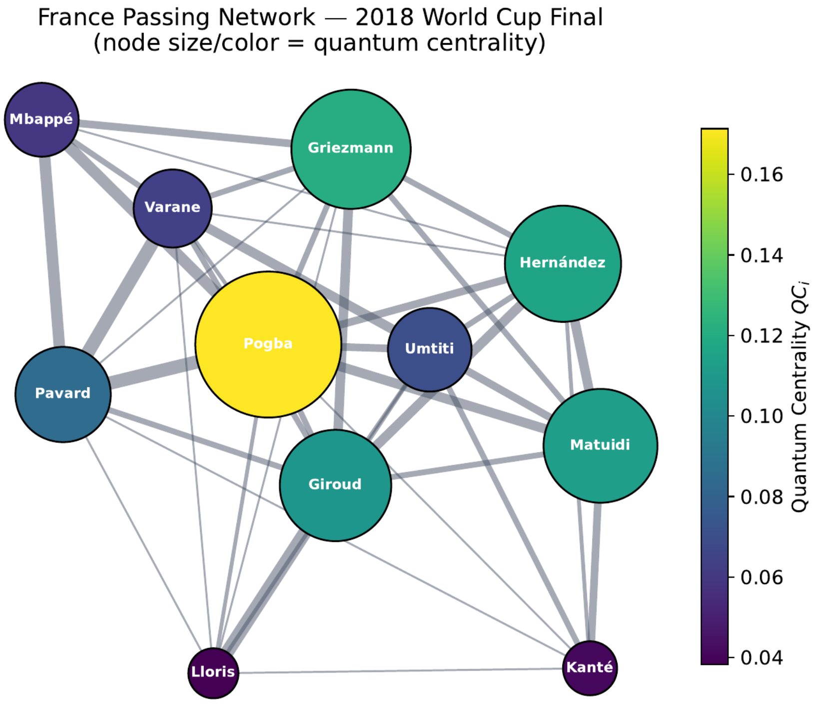

Figure 6. France's passing network for the 2018 World Cup Final.

8 | Discussion

The proposed construction is most useful as a transparent structural ranking of players within an event-derived network. Its outcome-prediction results are preliminary: the reported macro-AUC is only slightly above 0.5, the classical baseline has higher accuracy, and no uncertainty interval or statistical comparison is available. A full evaluation must retain the two teams from each match in the same fold and publish fold-level predictions, code, random seeds, and hyperparameters.

Several modeling limitations are important. First, StatsBomb Open Data are event data rather than continuous tracking data, so the defensive and spatial-progression layers are proxies. Second, the 15-minute windows, fuzzy thresholds, layer weights, and evolution-time grid are fixed a priori and need sensitivity analysis. Third, symmetrization is required for the present Hermitian Hamiltonian but removes pass direction. Fourth, selecting the 11 players with the most event touches may mix starters and substitutes and favor high-involvement players. Finally, a quantum-centrality ranking describes the supplied network representation; it does not by itself identify causal or match-decisive performance.

9 | Conclusion

This study developed a Temporal Multilayer Fuzzy Quantum Graph framework that combines fuzzy-weighted event layers with continuous-time quantum-walk centrality. A real-symmetric Hamiltonian ensures mathematically valid unitary evolution. Using the supplied 2018 FIFA World Cup analysis, the method produces structural player rankings; in the Final case study, Paul Pogba received France's highest quantum-centrality score.

Table 3. Quantum centrality ranking, France, 2018 World Cup Final.

Rank	Player	Quantum Centrality QC_i
1	Paul Pogba	0.1713
2	Antoine Griezmann	0.1211
3	Lucas Hernández	0.1160
4	Blaise Matuidi	0.1122
5	Olivier Giroud	0.1083
6	Benjamin Pavard	0.0847
7	Samuel Umtiti	0.0700
8	Raphaël Varane	0.0637
9	Kylian Mbappé	0.0592
10	N'Golo Kanté	0.0413
11	Hugo Lloris	0.0383

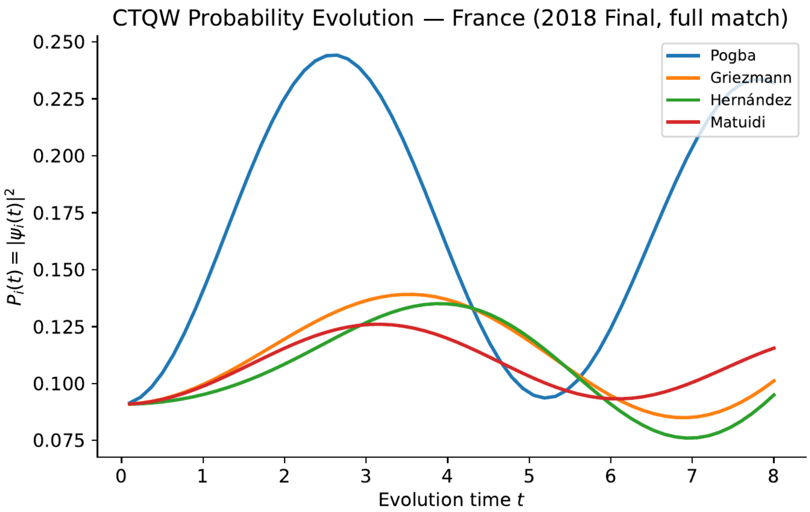

Figure 7. CTQW probability evolution $P_i(t)$ for France's four highest quantum-centrality players in the 2018 World Cup Final.

The outcome-prediction results remain exploratory and do not yet establish an advantage over classical centrality.

Future work should test multiple competitions, use match-grouped nested validation, publish a reproducible pipeline, analyze sensitivity to fuzzy and quantum parameters, and compare the method with classical temporal-network models and graph neural networks.

Author Contributions

All authors contributed equally.

Funding

The funding statement must be confirmed by all listed authors before publication.

Data Availability

The event data are publicly available from the StatsBomb Open Data repository cited above. The derived feature table, fold assignments, and analysis code were not included in the supplied source package and should be archived before publication.

Competing Interests

The competing-interests statement must be confirmed by all listed authors before publication.

Generative-AI Assistance

Generative AI assisted with language, LaTeX preparation and technical representation of the paper.

References

[1] Grund, T. U. (2012). Network structure and team performance: The case of English Premier League soccer teams. *Social networks,* 34(4), 682-690. https://doi.org/10.1016/j.socnet.2012.08.004

[2] Pena, J. L., & Touchette, H. (2012). *A network theory analysis of football strategies*. https://doi.org/10.48550/arXiv.1206.6904

[3] Clemente, F. M., Martins, F. M. L., & Mendes, R. S. (2016). *Social network analysis applied to team sports analysis*. Springer. https://doi.org/10.1007/978-3-319-25855-3

[4] Buldú, J. M., Busquets, J., Echegoyen, I., & Seirul. lo, F. (2019). Defining a historic football team: Using network science to analyze Guardiola's FC Barcelona. *Scientific reports, 9*(1), 13602. https://doi.org/10.1038/s41598-019-49969-2

[5] Buldú, J. M., Busquets, J., Martínez, J. H., Herrera-Diestra, J. L., Echegoyen, I., Galeano, J., & Luque, J. (2018). Using network science to analyse football passing networks: Dynamics, space, time, and the multilayer nature of the game. *Frontiers in psychology, 9*, 1900. https://doi.org/10.3389/fpsyg.2018.01900

[6] Farhi, E., & Gutmann, S. (1998). Quantum computation and decision trees. *Physical review A*, 58(2), 915. https://doi.org/10.1103/PhysRevA.58.915

[7] Childs, A. M. (2009). Universal computation by quantum walk. *Physical review letters, 102*(18), 180501. https://doi.org/10.1103/PhysRevLett.102.180501

[8] Izaac, J. A., Zhan, X., Bian, Z., Wang, K., Li, J., Wang, J. B., & Xue, P. (2017). Centrality measure based on continuous-time quantum walks and experimental realization. *Physical review A, 9*5(3), 032318. https://doi.org/10.1103/PhysRevA.95.032318

[9] Rossi, L., Torsello, A., & Hancock, E. R. (2014). Node centrality for continuous-time quantum walks. *Joint IAPR international workshops on statistical techniques in pattern recognition* (*SPR*) *and structural and syntactic pattern recognition* (*SSPR*) (pp. 103-112). Berlin, Heidelberg: Springer Berlin Heidelberg. https://doi.org/10.1007/978-3-662-44415-3_11

[10] Zadeh, L. A. (1965). Fuzzy sets. *Information and control,* 8(3), 338-353. https://doi.org/10.1016/S0019-9958(65)90241-X

[11] Rosenfeld, A. (1975). Fuzzy graphs. In *Fuzzy sets and their applications to cognitive and decision processes* (pp. 77-95). Academic Press. https://doi.org/10.1016/B978-0-12-775260-0.50008-6
[12] Tavana, M., Azizi, F., Azizi, F., & Behzadian, M. (2013). A fuzzy inference system with application to player selection and team formation in multi-player sports. *Sport management review, 16*(1), 97-110. https://doi.org/10.1016/j.smr.2012.06.002
[13] Duch, J., Waitzman, J. S., & Amaral, L. A. N. (2010). Quantifying the performance of individual players in a team activity. *PloS one,* 5(6), e10937. https://doi.org/10.1371/journal.pone.0010937
[14] Kivelä, M., Arenas, A., Barthelemy, M., Gleeson, J. P., Moreno, Y., & Porter, M. A. (2014). Multilayer networks. *Journal of complex networks, 2*(3), 203-271. https://doi.org/10.1093/comnet/cnu016
[15] Holme, P., & Saramäki, J. (2012). Temporal networks. *Physics reports,* 5*19*(3), 97-125. https://doi.org/10.1016/j.physrep.2012.03.001
[16] Ramos, J., Lopes, R. J., & Araújo, D. (2018). What's next in complex networks? Capturing the concept of attacking play in invasive team sports. *Sports medicine, 4*8(1), 17-28. https://doi.org/10.1007/s40279-017-0786-z
[17] StatsBomb. (2025). *StatsBomb open data* [*GitHub repository*]. https://github.com/statsbomb/open-data